

7

Abstract Submitted
for the Berkeley Meeting of the
American Physical Society
27-29 December 1973

Physical Review
Analytical Subject Index
Number 44.4

Bulletin Subject Heading
in which paper should be placed:
Electronic Structure and Optical
Properties.

Electronic Structure of Two Coupled Parallel
Conducting Chains. P. M. GRANT, IBM Research Labora-
tory, San Jose, Calif. A simple nearest neighbor
tight-binding model is used to discuss the itinerant
electronic structure of two parallel interacting
conducting chains. This model may be relevant to the
organic conductor (TTF)(TCNQ) where parallel stacking
of the cations and anions approximates the system
above. Emphasis will be placed on the role of band
interaction in determining optical properties, partic-
ularly plasma frequencies.

Submitted by

Paul M. Grant

Paul M. Grant
IBM Research Laboratory
San Jose, Calif. 95193

bulletin

OF THE AMERICAN PHYSICAL SOCIETY

1 DECEMBER 1973

1973 WINTER MEETING IN THE WEST
IN BERKELEY, CALIFORNIA
27-29 DECEMBER 1973

MGR166160 BAPS 018012 10
PAUL M GRANT
I B M RESEARCH LABS
MONTEREY & COTTLE RDS
SAN JOSE CA 95193

SERIES II VOLUME 18 NUMBER 12 • BERKELEY, CALIF. • 1 DECEMBER 1973 • PAGES 1561-1628

PUBLISHED FOR THE AMERICAN PHYSICAL SOCIETY
BY THE AMERICAN INSTITUTE OF PHYSICS

965-118M-101

(LEO M. FALICOV presiding)

Electronic Structure. TCNQ

BD 1 Electronic Structure of Two Coupled Parallel Conducting Chains. P. M. GRANT, IBM Research Laboratory, San Jose, Calif. A simple nearest neighbor tight-binding model is used to discuss the itinerant electronic structure of two parallel interacting conducting chains. This model may be relevant to the organic conductor (TTF)(TCNQ) where parallel stacking of the cations and anions approximates the system above. Emphasis will be placed on the role of band interaction in determining optical properties, particularly plasma frequencies.

BD 2 RAMAN SCATTERING BY SURFACE POLARITONS I. THEORY. Y. J. Chen and E. Burstein, Univ. of Penna., and D. L. Mills, Univ. of Calif.--We have obtained macroscopic expressions for the Raman scattering cross-section of surface polaritons ($s\pi$) at single interface and two interface (thin slab) configurations. Differences from the expressions for TO and LO phonons arise from the exponential attenuation of the surface modes [$\exp(-\alpha z)$] away from the interface. In the single interface case, the scattering cross-section of $s\pi$ can be comparable to that of TO and LO phonons only when the non-linear (NL) medium (not necessarily the surface active medium) is "opaque" and the skin depth for the exciting radiation is comparable to the penetration depth $1/\alpha$ of the $s\pi$ in the NL medium. In the two interface case the $s\pi$ scattering cross-section is an oscillatory function of the slab thickness d . Apart from this aspect and the cancellation of contributions from different regions of the slab, the $s\pi$ scattering cross-section can be comparable to that of TO and LO phonons, particularly in forward scattering, when the slab is NL and $d \leq 1/\alpha$.

BD 3 OBSERVATION OF MAGNETOPLASMON-TYPE SURFACE POLARITONS ON n-InSb. A. Hartstein and E. Burstein Univ. of Penna., and E. Palik, U.S. Naval Res. Lab.--We have observed magneto-plasmon-type surface polaritons at n-type InSb-air interfaces in an external magnetic field using the ATR method. The experiments were carried out for the Voigt configuration ($k \perp E_0$) with E_0 oriented perpendicular to the sagittal plane. Two values of the carrier concentration were used in order to study the surface polaritons in the regions of both strong and weak LO phonon-plasmon coupling. The data are in good qualitative agreement with theory. In particular, they confirm the non-reciprocal nature of the dispersion curves and the appearance of the virtual excitation type branches. On the basis of data obtained in zero magnetic field on etched surfaces, the quantitative differences between experimental and theoretical dispersion curves are attributed to surface damage.

BD 4 Dispersion of Nonlinear Optical Susceptibility $\chi^{(2)}(2\omega)$ of III-V Semiconductors.^{*} D. BETHUNE, A. J. SCHMIDT, and Y. R. SHEN, Dept. Phys., Univ. of Calif., Berkeley, and IMRD, Lawrence Berkeley Lab., Berkeley, Calif.--We report the results of our measurements on the nonlinear optical susceptibility $\chi^{(2)}(2\omega)$ of GaAs, InAs, and InSb at 80°K and 300°K using a flashlamp-pumped-dye laser. The fundamental frequency varies from 1.8 to 2.8 eV. Our results therefore complement those earlier results of Parsons and Chang¹ using a ruby-laser-pumped dye laser. In this region, either ω or 2ω appears in resonance with a number of known critical points. We shall compare our experimental results with

theoretical predictions from the available band structures of these compounds. Possible enhancement of $\chi^{(2)}(2\omega)$ due to double resonance will be discussed.

* Work supported by the U.S. Atomic Energy Commission. I. F. G. Parsons and R. K. Chang, Optics Comm. **3**, 173 (1971).

BD 5 The Preparation and Characterization of TTF-TCNQ Thin Films. T. H. CHEN* and B. H. SCHECHTMAN, IBM Research Laboratory, San Jose, Calif.--Thin films of the highly conducting organic complex tetrathiofulvalinium-tetracyanoquinodimethane (TTF-TCNQ) have been successfully deposited using conventional thermal evaporation techniques. Films ranging from 0.2 to 4 μ thick have been grown under varied conditions of substrate material, substrate temperature, and source temperature. Spectroscopic, electrical and differential thermal studies and chemical elemental analysis have been performed to chemically characterize the films. Scanning electron microscopy and x-ray diffractometry were applied to characterize the surface topography and the polycrystalline structure of the films, and to correlate the structure with optical and electrical observations. Typical electrical conductivity of the films at room temperature is $10(\text{ohm-cm})^{-1}$ and it decreases with decreasing temperature. Although grain boundary barrier activation precludes observation of a metallic temperature dependence, the single crystal metal-insulator transition near 60° K is exhibited in the films as an abrupt change in the temperature dependence of the conductivity.

*Permanent address: Chem. Dept., U. C. Berkeley, CA.

BD 6 Orientalional Peierls Transition In Organic Conductors. H. MORAWITZ, IBM Research Lab.--I consider a model of planar molecules forming a one-dimensional stack with a partially filled π -electron conduction band in the tight-binding approximation. I show that electron-phonon coupling leads to an orientational Peierls transition connected with the softening of the librational mode. Below the orientational transition temperature the order parameter is a finite angle of rotation, corresponding to macroscopic occupation of the librational mode. Implications of this model for the metal-insulator transition in TTF-TCNQ will be discussed and an experimental test of this model will be proposed.

BD 7 Energy Band Calculations on Linear Chain Transition Metal Complexes.^{*,†} A. ABARBANEL, Stanford U.--The KKR formalism was adapted to handle the band structure of a linear chain platinum compound prototypic of the class of mixed valence platinum linear chain compounds.¹ A zero order non relativistic computation was carried out and several approximation schemes developed. Energy band structures for the d-electrons of the central platinum atoms were computed for several intermetallic separations and for several charge distributions within the unit cell (to stimulate the effects of differently sized and charged ligands to the platinum atoms in actual compounds). Several refinements including more rigorous handling of the crystal potential and implementation of a relativistic formulation are discussed.

*Submitted by W. A. LITTLE.

†Supported by Advanced Research Projects Agency through the Center for Materials Research.

¹K. Kroghmann, Angew. Chem. Int. Ed. Engl. **8**, 35 (1969).

INTRODUCTION

In this talk, we're going to examine some of the physical consequences of a simple one-electron tight-binding model applied to a quasi-one-dimensional system of interacting parallel conducting chains. The motivation for investigating such a model arises from its possible application to the radical cation-anion charge transfer salt (TTF)(TCNQ). Here the TTF⁺ and TCNQ⁻ ions form parallel odd-electron stacks and Perlstein and Bloch of the Johns Hopkins group have suggested that the electronic structure of the solid may indeed arise from overlap of the conduction bands based on each stack.

Our approach will be to derive the Fermiology of such a model and discuss in particular the relationship between the Drude plasma frequency and the various band parameters involved. Greene, Wrighton, Castro and myself, and Bright, Garito and Heeger have recently measured the near-IR optical properties of (TTF)(TCNQ) and it is important to understand how to interpret the experimental results should an overlapping band model apply.

We will also discuss briefly why the model may explain the current difficulty in observing directly a Peierls distortion in (TTF)(TCNQ) and in addition touch on how really relevant this purely itinerant model is to such materials.

FIRST SLIDE

The first slide gives the model details explicitly. We have two alternating chains of molecules, A and B, which we will assume bonded by p-pi type bonds along the chain direction, x, and by inter-MO p-sigma type bonds in the interchain direction, y. The assumption of these particular bonds is merely for purposes of setting symmetry and notation conventions and we don't mean to imply such simple bonds really describe a given material like (TTF) (TCNQ).

The nearest-neighbor tight-binding secular equation appears as shown with t_{AA} and t_{BB} being the intrachain transfer integrals along what will become the conducting direction. The interchain coupling term is given by t_{AB} .

Note first the solution on the $k_y = \pi/b$ Brillouin zone face. Here we have just the diagonal terms of the secular determinant giving two tight-binding bands of familiar form separated by an energy α and with widths $4t_{AA}$ and $4t_{BB}$. The interplay of α and the bandwidths determines of course the amount of band overlap.

Next note the solution on the $k_x = 0$ plane along k_y in the interchain direction. The bandwidth now involves band separation as well as the transfer integral. In the event α is much greater than t_{AB} , the case we are really interested in, the

interchain bandwidth is simply $4(t_{AB}^2)/\alpha$.

Although the model is two-dimensional, we will refer to such artifices as Fermi surfaces and k-space volumes even though they are strictly lines and areas.

SECOND SLIDE

Let's flesh the model out by putting in some numbers appropriate to weak interchain coupling. Next slide, please.

Here we have chosen the interchain coupling to be about an order of magnitude less than that along the chain. The choice of $\alpha=1.6\text{eV}$ assures considerable band overlap. The results are clearly seen in the traces of the bands on the $k_y=\pi/b$ and $k_x=0$ planes. The interchain bands are much narrower than the intrachain bands, especially when one sees the difference in energy scales between the k_x and k_y figures.

If we assume an electron population density such that the Fermi level is at 3eV thus intersecting both bands, then the root loci of our secular determinant yield the two Fermi surfaces, one for each band, shown in the lower diagrams. Here we have plotted only the upper right hand quadrant of the Brillouin zone with the k_x scale expanded to display the surface curvature. It is easy to see that in the limit of weak interchain coupling, the family of Fermi surfaces degenerates into a set of parallel lines (parallel planes in 3D) perpendicular to k_x .

THIRD SLIDE

In order to apply the model to experimental situations, we must establish the Fermi energy in terms of the tight-binding parameters. This is done on the next slide through use of the standard relation defining electron density in terms of integrals over k-space volumes underneath Fermi surfaces. For overlapping bands we can have two such integrals as shown.

For t_{AB} much less than both t_{AA} and t_{BB} , and for 2 electrons per unit cell, one from molecule A and one from B, carrying out the integration leads to the rather obvious fact that the respective Fermi vectors must sum to π/a . Using this result and the following two equations from the diagonal elements of the secular equation, we obtain the Fermi energy in terms of bandwidths and band separation.

Before going on, let's make a few remarks regarding (TTF)(TCNQ). Suppose the B-band arises from the TTF ion chain and the A-band from TCNQ. In counting the number of bonding electrons per unit cell we find the figure is even. The problem of determining the cation-anion charge transfer state is then the same (on a strictly one-electron picture) as establishing the amount of band overlap. That is, if the two bands don't overlap at all, then both TTF and TCNQ are doubly ionized and all electrons reside in a completely filled TCNQ band and we have an insulating state. If the overlap

is such that the centers of each band coincide, they are then each half-full and we have singly ionized TTF and TCNQ and a strongly metallic state. On the other hand, if the bands completely cross so that the TTF band lies entirely below TCNQ, then no charge transfer takes place, the cation and anion remain neutral, and we again have an insulating state.

Current experimental evidence seems to indicate single ionization as the most likely situation in (TTF)(TCNQ). Glen Wrighton, in his talk later this session, will show optical data revealing TCNQ- structure in the solid, and Warren Grobman and his collaborators at IBM Yorktown are interpreting their photoemission and ESCA results on the basis of single electron charge transfer also. On a strictly itinerant one-electron picture such as we have been discussing, we would have to have perfectly overlapping bands. However, if coulomb repulsion effects are important, it would be possible for the bands to still be half-filled with finite separation. An obvious extension of the present work would be the study of coupled Hubbard chains.

One more point and this concerns the question of the Peierls distortion purportedly responsible for the metal-insulator transition in (TTF)(TCNQ). We can see that, given some arbitrary band overlap, the period of the distortion necessary to break the Fermi level degeneracy may be very poorly commensurate with the

chain period. This situation would make the direct detection of the distortion by diffraction techniques difficult.

FOURTH SLIDE

Finally, let's touch on the way one physically measurable quantity, namely, the Drude plasma edge, depends on the parameters of two overlapping tight-binding bands. This is summarized on the next slide.

The first equation states the dielectric function as the sum of two Drude terms, one for each band, with the plasma frequencies given by a Fermi surface integral of the indicated form. Working out these integrals explicitly for our model yields the two expressions you see next in terms of the respective bandwidths and band separations.

Now, if the Drude scattering times are the same for both bands, or longer than the period of the incident radiation, then the squared plasma frequencies can be summed. Furthermore, if the bandwidths are nearly equal, and we define a band overlap energy as shown, Z then the squared plasma frequency becomes proportional to the geometric mean of band overlap and band separation. But, if the overlap is perfect, then the squared plasma frequency goes as the sum (not average) of the two bandwidths.

The lesson to be learned from this discussion is that one can't simply interpret plasma energies in a situation where band overlap might apply (as one can for a single tight-binding band) without

some external knowledge of the overlap features of the band structure.

CONCLUSION

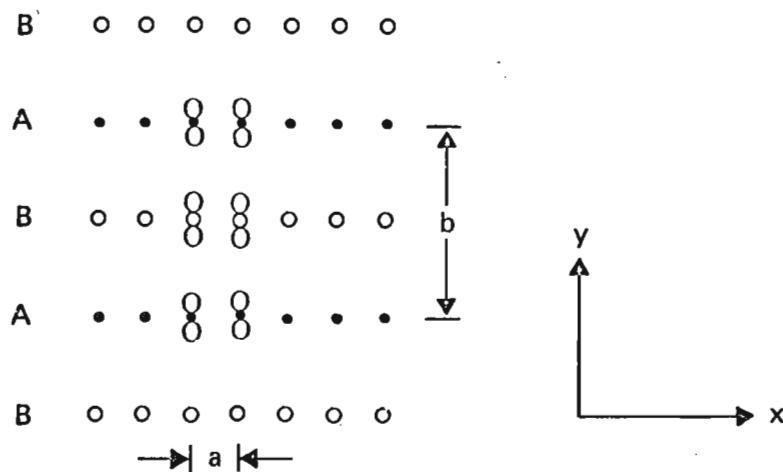
We conclude with the three comments summarized on the fifth and final slide:

The overlapping band model may apply to (TTF)(TCNQ) although it would be obviated if intrachain coulomb repulsion energies turned out to be of the order of the bandwidths.

If it is applicable, the arbitrariness of the overlap may lead to poor commensurability making direct observation of the Peierls distortion problematical.

Lastly, in order to settle the applicability issue, experiments should be performed to test for the presence of holes and to determine directly the majority and minority carrier concentrations in (TTF)(TCNQ). However, the classical experiments in this area, such as Hall and deHaas-Van Alphen measurements, may prove very difficult to interpret in this highly anisotropic system.

Coupled Tight-Binding Chains



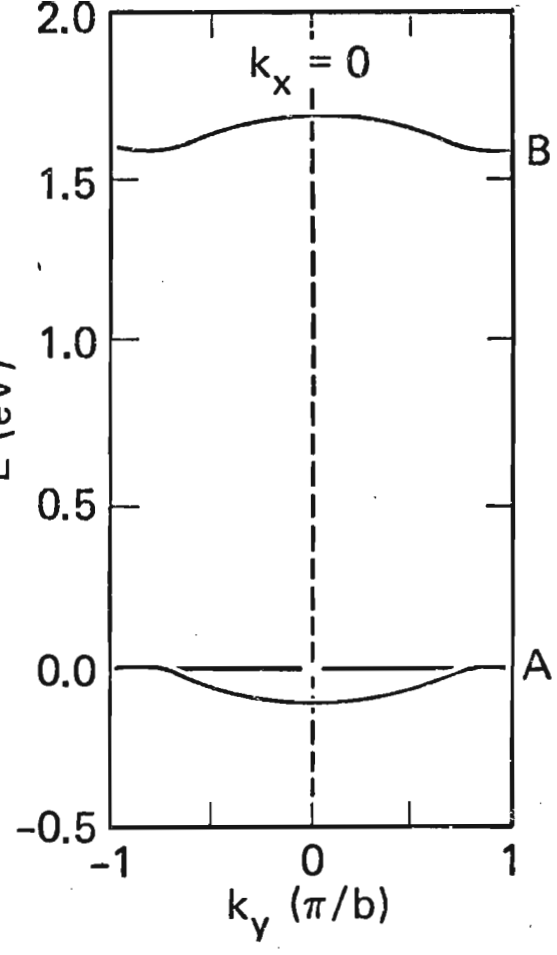
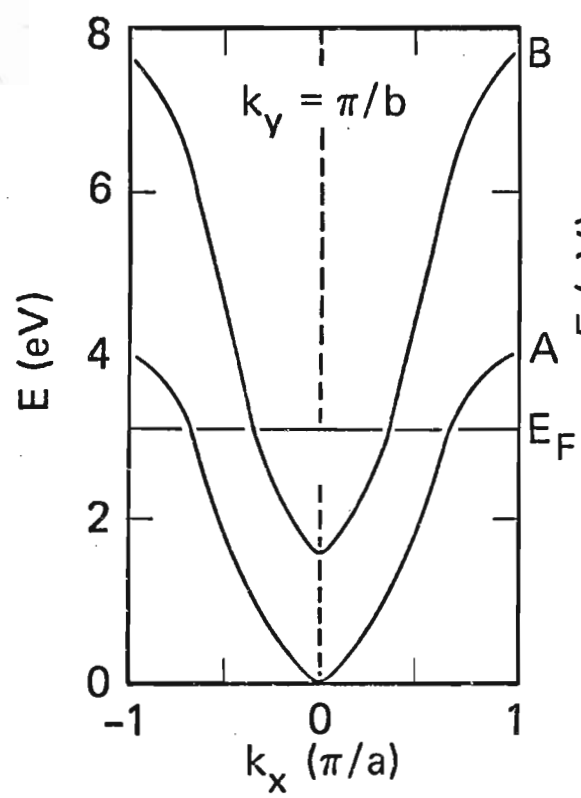
$$\begin{vmatrix} -E_k + 2t_{AA}(1 - \cos k_x a) & -2t_{AB} \cos k_y b/2 \\ -2t_{AB}^* \cos k_y b/2 & -E_k + \alpha + 2t_{BB}(1 - \cos k_x a) \end{vmatrix} = 0$$

$$k_x = 0: E_k = \frac{\alpha}{2} \left\{ 1 \pm \left[1 + \frac{16 t_{AB}^2}{\alpha^2} \cos^2 k_y b/2 \right]^{1/2} \right\}$$

$$\text{Interchain Bandwidth: } BW_{AB} = \frac{\alpha}{2} \left\{ \left[1 + \frac{16 t_{AB}^2}{\alpha^2} \right]^{1/2} - 1 \right\}$$

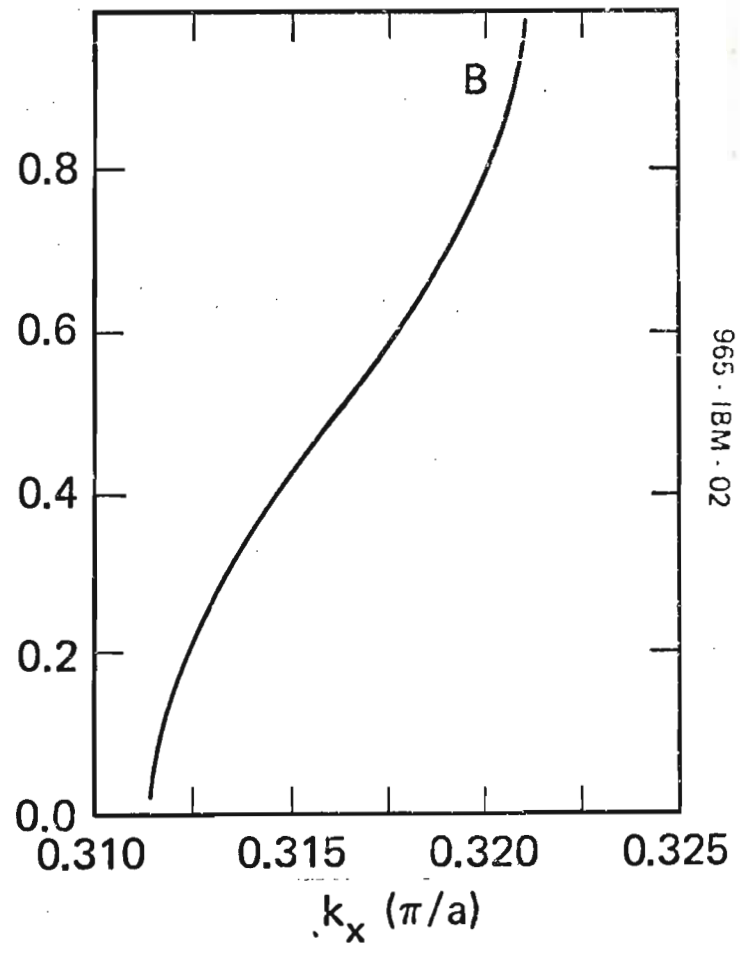
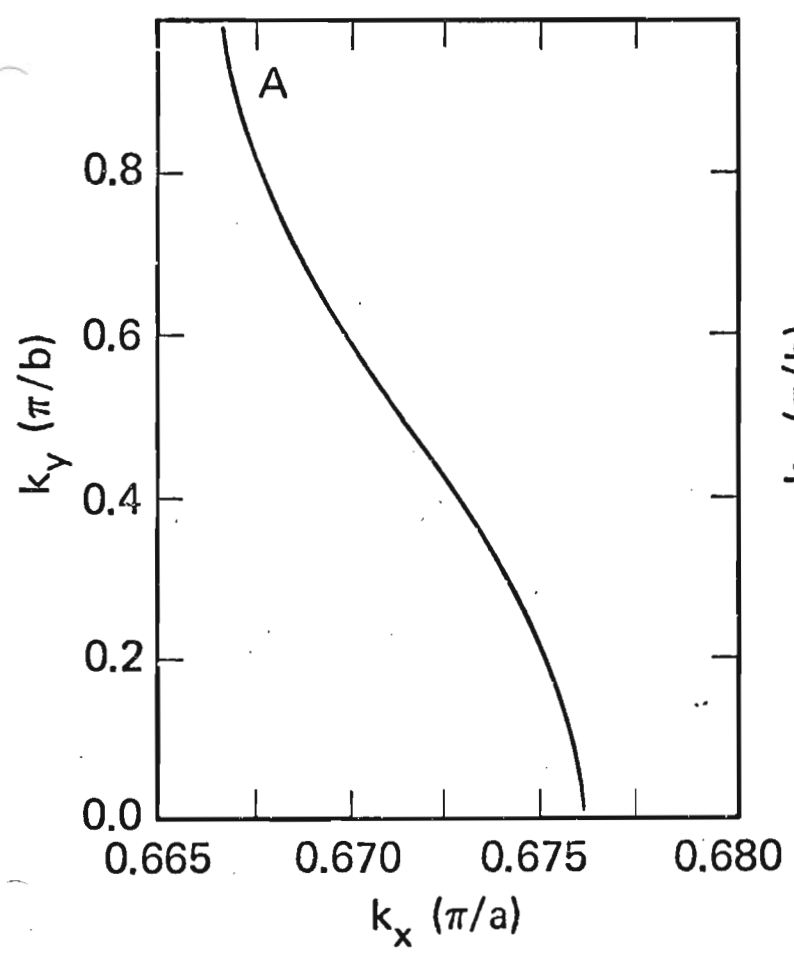
Band Structure

965 · IBM · 02



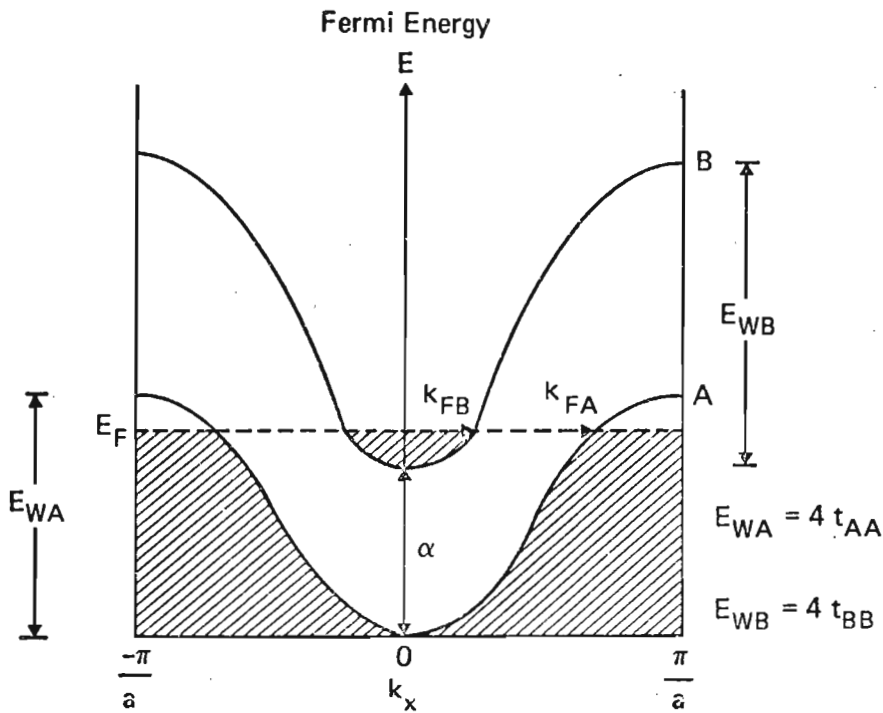
$t_{AA} = 1.0$
 $t_{BB} = 1.5$
 $t_{AB} = 0.2$
 $\alpha = 1.6$
 $E_F = 3.0$

} eV



965 · IBM · 02

Fermi Surfaces



Electron Density: $n = \frac{2}{4\pi^2} \left[\int_{V_A} dk_x dk_y + \int_{V_B} dk_x dk_y \right]$

For $t_{AB} \ll t_{AA}, t_{BB}$ and $n = 2/ab$:

$$k_{FA} + k_{FB} = \pi/a$$

$$k_{FA} = (1/a) \cos^{-1} \left(1 - 2 \frac{E_F}{E_{WA}} \right)$$

$$k_{FB} = (1/a) \cos^{-1} \left(1 - 2 \frac{E_F - \alpha}{E_{WB}} \right)$$

$$E_F = \frac{E_{WA}}{E_{WA} + E_{WB}} (E_{WB} + \alpha)$$

Optical Plasma Energies

$$\epsilon = 1 - \frac{\omega_{PA}^2}{\omega(\omega + i/\tau_A)} - \frac{\omega_{PB}^2}{\omega(\omega + i/\tau_B)}$$

$$\omega_P^2 \propto \int_{E_F} v dS_F$$

$$\omega_{PA}^2 = \frac{8e^2 a^2}{\hbar^2 v_a} \left[\frac{E_{WA}}{E_{WB} + E_{WB}} \left\{ (E_{WA} - \alpha)(E_{WB} + \alpha) \right\}^{1/2} \right]$$

$$\omega_{PB}^2 = \frac{8e^2 a^2}{\hbar^2 v_a} \left[\frac{E_{WB}}{E_{WB} + E_{WA}} \left\{ (E_{WA} - \alpha)(E_{WB} + \alpha) \right\}^{1/2} \right]$$

$$\omega_{PB}^2 / \omega_{PA}^2 = E_{WB} / E_{WA}$$

1. If $\tau_A = \tau_B$, $\omega_P^2 \sim \left\{ (E_{WA} - \alpha)(E_{WB} + \alpha) \right\}^{1/2}$
2. If $E_{WA} = E_{WB} = E_W$, $\omega_P^2 \sim (E_W^2 - \alpha^2)^{1/2}$
3. If $E_0 \ll \alpha$, where $E_0 \equiv E_W - \alpha$, $\omega_P^2 \sim (2\alpha E_0)^{1/2}$
4. Perfect Overlap: $\omega_P^2 \sim E_{WA} + E_{WB}$

CONCLUSIONS

- MODEL MAY APPLY TO RADICAL CATION-ANION CHARGE TRANSFER COMPLEXES LIKE (TTF) (TCNQ).
- OVERLAP MAY LEAD TO POOR COMMENSURABILITY MAKING OBSERVATION OF PEIERLS DISTORTION DIFFICULT.
- EXPERIMENTS MUST BE PERFORMED WHICH PROBE FERMI SURFACE FEATURES OF CATION-ANION CHARGE TRANSFER COMPLEXES.